Published OnlineFirst December 30, 2016; DOI: 10.1158/1541-7786.MCR-16-0286-T

Molecular Cancer Research

Immunophenotyping and Transcriptomic Outcomes in PDX-Derived TNBC Tissue

Eileen Snowden[1], Warren Porter[1], Friedrich Hahn[1], Mitchell Ferguson[1], Frances Tong[1], Joel S. Parker[2,3], Aaron Middlebrook[4], Smita Ghanekar[4], W. Shannon Dillmore[1], and Rainer Blaesius[1]

Abstract

Cancer tissue functions as an ecosystem of a diverse set of cells that interact in a complex tumor microenvironment. Genomic tools applied to biopsies in bulk fail to account for this tumor heterogeneity, whereas single-cell imaging methods limit the number of cells which can be assessed or are very resource intensive. The current study presents methods based on flow cytometric analysis and cell sorting using known cell surface markers (CXCR4/CD184, CD24, THY1/CD90) to identify and interrogate distinct groups of cells in triple-negative breast cancer clinical biopsy specimens from patient-derived xenograft (PDX) models. The results demonstrate that flow cytometric analysis allows a relevant subgrouping of cancer tissue and that sorting of these subgroups provides insights into cancer cell populations with unique, reproducible, and functionally divergent gene expression profiles. The discovery of a drug resistance signature implies that uncovering the functional interaction between these populations will lead to deeper understanding of cancer progression and drug response.

Implications: PDX-derived human breast cancer tissue was investigated at the single-cell level, and cell subpopulations defined by surface markers were identified which suggest specific roles for distinct cellular compartments within a solid tumor. *Mol Cancer Res; 1–10. ©2016 AACR.*

Introduction

Cancer tissue is—like any tissue—by nature an ecosystem formed by a variety of phenotypically distinct cells. With the recognition of cancer as a genetic disease a few decades ago, the focus of drug discovery efforts almost sidelined these differences in the hope that the genetic differences between "healthy" and "diseased" would provide sufficient information to develop effective therapeutics and associated diagnostic tools to choose those drugs (1). Even today most molecular diagnostic tests treat tissue as a bulk entity from which a single genotype is determined in order to categorize the disease, derive a prognosis, and decide on the optimal therapy. As a plethora of targeted drugs were developed, a fast growing number of clinical trials led to increased progression-free survival while often reducing side effects compared with traditional chemotherapy or radiotherapy (2). While this lent preliminary confirmation to the general approach of aiming at one molecularly defined target, the hopes for a major improvement in overall survival were severely dampened as the clinical trials continued to show that increased survival time was almost invariably followed by relapse and emergence of drug resistance. Relapse, and in the large majority of cases concomitant metastasis, continues to be the main cause of mortality for many cancer types (2).

The role of the tumor microenvironment (TME) which has a strong influence on tumor fate (3) as well as the development of the cancer stem cell (CSC) model (4–6) offered arguments not to rely on a too simplistic tumorigenesis model and also the motivation to include phenotypic cellular differences in the investigation of cancer tissue. Deep phenotypic analysis of tumor-associated immune cells provides ample evidence that valuable information can be elucidated regarding the TME from cells embedded in and surrounding a cancer lesion (7). The initially rather static CSC concept was refined through the realization that even cells initially classified as nonstem cells can adopt a stem cell phenotype (8), and recent models indicate that the view of cells able to switch between various degrees of "stemness" may be more accurate (9).

The arguments for inclusion of phenotypic differences grew even stronger with a better recognition of a second source of intratumor heterogeneity (ITH)—in addition to TME cells colocalized with neoplastic cells—which develops as a consequence of cancer evolution. The basic concept of cancer evolution was defined almost 40 years ago (10), and several noteworthy experiments were carried out to investigate interactions between subclonal populations within a tumor (11). Partly due to technical limitations, ITH remained on the periphery for the next three

[1]BD Technologies, Research Triangle Park, Durham, North Carolina. [2]Lineberger Comprehensive Cancer Center, University of North Carolina, Chapel Hill, North Carolina. [3]Department of Genetics, University of North Carolina, Chapel Hill, North Carolina. [4]BD Biosciences, San Jose, California.

Note: Supplementary data for this article are available at Molecular Cancer Research Online (http://mcr.aacrjournals.org/).

E. Snowden and W. Porter contributed equally to this article.

Some tumor data for this paper were retrieved from the Mouse Tumor Biology Database (MTB), Mouse Genome Informatics, The Jackson Laboratory, Bar Harbor, Maine. http://www.informatics.jax.org. (October, 1998 i.e., data retrieved 8/4/16).

Corresponding Author: Rainer Blaesius, BD Technologies, 21 Davis Dr, Research Triangle Park, NC 27709. Phone: 919-597-6620; Fax: 919-597-6400; E-mail: rblaesius@bd.com

doi: 10.1158/1541-7786.MCR-16-0286-T

Published OnlineFirst December 30, 2016; DOI: 10.1158/1541-7786.MCR-16-0286-T

decades. Observations of correlation between high ITH and poor prognosis in Esophageal cancer where evidence of heterogeneity was more easily accessible (12) revived this "dormant" branch of cancer research. Over the last decade, it has become clear that ITH is not just a peculiar side effect but likely reflects essential mechanisms enabling a tumor to react to dynamic selective pressures caused by the immune system, hypoxia, cancer drugs, and other environmental pressures (12, 13). Discovery of extensive genetic and transcriptional heterogeneity (14, 15) added necessary functional aspects to the model which has since been widely accepted. Finally, very compelling arguments for the clinical importance of an ITH-based model come from data tying heterogeneity to outcome across at least nine cancer types (16) as well as to major mechanisms of drug resistance either in the form of pre-existing resistant subclones or through *de novo* adaptive resistance driven by evolutionary mechanisms (17–19).

Image-based methods can reveal the presence of phenotypically different cells in tissue. Metrics to assess ITH based on imaging have also been developed (20), but while they allow basic quantification of the degree of ITH, their restrictions in sampling (one slice at a time) and number of measured parameters as well as the lack of downstream analysis options severely limit the depth of information extractable from a biopsy. Separation of cells according to specific properties prior to applying downstream analysis methods, such as next generation sequencing, gene expression, epigenetics, and other "omics," on the other hand provides much deeper insight. Blood-borne cancers for example provide evidence that subclones display functional differences between each other when tested in mouse tumor models (21). Once identified, such subpopulations can be subjected to downstream analysis to elucidate cellular function (22). Some large-scale screening campaigns of cancer cell lines identified a range of potential surface markers that can be used in this fashion (23). More systematic tools and methods are urgently needed to make this approach accessible to research and clinical laboratories investigating solid tumor biopsies, and a more refined understanding of heterogeneity is necessary to positively affect patient care (24).

To assess solid tumor heterogeneity in human breast cancer, we established a workflow to extract tissue biopsies, dissociate the cells, and subject them to flow cytometric analysis and sorting (Fig. 1). We generated surface marker profiles of biopsies obtained from patient-derived xenograft (PDX) mouse breast cancer models using a range of reported CSC markers (4, 25–27). CD24 and CD44 as the earliest reported breast CSC markers (4, 25) and ERBB2 (HER2) as prominent breast cancer target reported to show different expression levels on the surface of breast cancer cells (28) were obvious choices to include in our panels. ITGA6 (CD49f), CD90, PROM1 (CD133), CD184, and EPCAM (CD326) have been found to be heterogeneously expressed in breast cancer cell lines (26). ITGB1 (CD29) was reported to have a role in breast cancer metastasis (29), and ALCAM (CD166) was also found to be associated with breast CSCs (30). Our results provide a profiling tool potentially complementing existing breast cancer molecular subtyping systems. Despite showing some value in predicting therapy responses, the systems in use are still limited in their accuracy, and improvements are needed, especially in triple-negative breast cancers (28, 31). To investigate whether the variation in surface markers reflects an underlying phenotypic divergence, we sorted cells from triple-negative breast cancer PDX mice and discovered evidence for profound differences in the expression profile of two distinct subpopulations.

Our results suggest that flow cytometry provides a useful tool for characterization of solid tumor biopsies and can serve as a basis to identify multiple tumor cell subpopulations of interest.

Materials and Methods

The PDX mouse tumor model system provides a renewable source of human tumor tissue displaying similar tissue structures as clinical material (32, 33). Mice were sourced from The Jackson Laboratory. The properties of the mouse cohorts used in the study are listed in Table 1.

PDX tumor extraction

Female NOD/SCID/ILIIrg$^{-/-}$ (NSG) mice age 6 to 7 weeks were purchased from The Jackson Laboratory with tumor material already implanted. All animal studies were performed under an Institutional Animal Care and Use Committee–approved protocol. Tumors were assessed weekly for growth and measured with a digital caliper. Tumor volume was estimated by the formula $0.5 \times (\text{length} \times \text{width}^2)$. Once tumor size reached >500 mm^3 (several weeks to several months), they were harvested for analysis. Mice were humanely euthanized, and the tumor was immediately removed via blunt dissection and placed in cold PBS for dissociation and analysis.

Preparation of single-cell suspensions from tumor tissue

Excised tissue was weighed and then minced using a scalpel or scissors to a size not exceeding 1 to 2 mm^3. Tissue was then enzymatically dissociated into single cells as previously described (34–36) in a 37°C water bath for 30 minutes with frequent agitation. The enzymatic reaction was stopped by rinsing in PBS (Cellgro) and 1% BSA (Sigma-Aldrich). Dissociated tissue was filtered through a 70 μm sieve and treated with ACK Buffer (Life Technologies) to remove contaminating red

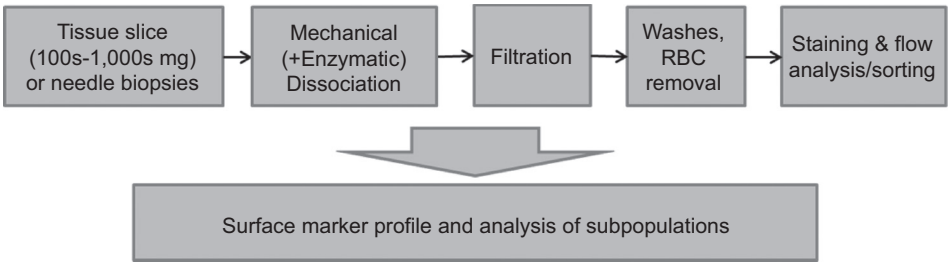

Figure 1.
Work flow for sample preparation. Tumor tissue resections from PDX mice were dissociated and subjected to flow cytometric analysis or sorting followed by RNASeq. Immunophenotyping can also identify populations for use in other (−omics) or functional methods.

Published OnlineFirst December 30, 2016; DOI: 10.1158/1541-7786.MCR-16-0286-T

Table 1. Breast cancer PDX mouse cohorts used

Name	Description	ER	PR	Her2	Passage	*N*	JAX Labs Des.
BRC3[a]	Mixed ductal carcinoma; lung metastasis	–	–	–	3	7	TM00096[a]
BRC4	IDC	–	–	–	4	6	TM00099
BRC5	IDC	+	+	–	1	5	TM00991
BRC7	Carcinoma/BRCA1$^+$	–	–	–	3	4	TM00089
BRC8	IDC	–	–	–	4	10	TM00090
BRC9	IDC/BRCA1$^+$	–	–	–	4	10	TM00091
BRC10	IDC/Her2$^+$	–	–	+	2	4	TM00129
BRC12[a]	Mixed ductal carcinoma; lung metastasis	–	–	–	4	8	TM00096[a]
BRC13	IDC	–	–	–	4	7	TM00999

NOTE: Clinical information for patient sample used to create tumor model retrieved from The Jackson Laboratory website http://tumor.informatics.jax.org/mtbwi/pdxSearch.do 8/4/16 where additional pathology data can be found.
[a]Note that BRC3 and 12 are different passages of the same tumor model.

blood cells. Cells were resuspended in PBS, without magnesium and calcium.

Cell staining for flow cytometry and analysis

Before staining, single-cell suspensions were blocked for 30 minutes, on ice in FcR block (Miltenyi Biotec). For surface marker characterization, cells were diluted in PBS and distributed into wells of a 96-well plate containing viability dye (LIVE/DEAD Fixable Near-IR or Aqua, Invitrogen) and Hoechst 33342 (Invitrogen; at 0.2 μg/mL) for viable nucleated cell identification. Monoclonal antibodies used are listed in Table 2.

Cells were incubated with antibody solutions for 30 minutes at 4°C, in the dark, and then rinsed twice in PBS before acquisition on BD LSRII flow cytometer. For sorting, cells were stained using a four-color panel combining amine viability reagent, anti-mouse cocktail, and markers identified from the primary characterization plate. After staining, cells were rinsed, and resuspended in BD FACS Pre-Sort Buffer, filtered again through a 70 μm sieve, and populations of interest were sorted on the BD FACSAria II (BD Biosciences) at 20 p.s.i. using a 100-μm nozzle. Cell doublets or clumps were removed with electronic doublet discrimination gating. Post-sorting analysis of sorted subpopulations regularly showed purity >95%. Analysis of results was performed using FACSDiva software (version 6.1.3 LSRll and version 8.0 FACSAria II). For gating strategy, see Supplementary Fig. S1.

Graphical representations of the data, cluster analysis, and calculation of two-way correlations (Figs. 2–5) were performed using R (37).

RNA isolation and RNASeq

A total of 80,000 or more cells chosen for a specific surface marker status were collected and processed for RNA extraction. Quality assessments were determined using Agilent BioAnalyzer and NanoDrop readings. RNA specimens underwent analysis to determine their suitability for target labeling. Analyses included determination of concentration and volume, A260/A280 ratio, and 28S/18S rRNA ratio (where applicable), and an RNA integrity summary score (Agilent RIN or Caliper RQS). RNASeq was performed using the Illumina RNASeq TruSeq Stranded mRNA SQ905 Kit. For comparison with other breast cancer gene expression profiles, a collection of 1,033 breast cancer samples was used as reference dataset (38). Pathway analysis based on the RNASeq data for the two cell populations sorted with CD184 was performed using PathVisio3 (39, 40). Significant biological functions were determined using the elim method of

Table 2. List of monoclonal antibodies used

Target	Fluorophore	Vendor	Catalogue number	Clone
CD326	PerCP-Cy5.5	BDB	347199	EBA-1
CD24	PE-CF594	BDB	562405	ML5
CD44	Alexa Fluor 700	BDB	561289	G44-26
CD45	APC-H7	BDB	560178	HI30
CD90	PE-Cy7	BDB	561558	5E10
CD49f	BV421	BDB	562582	GoH3
HER-2/neu	PE	BDB	340552	Neu 24.7
CD133/1	APC	Mil	130-090-826	na
CD166	PE	BDB	559263	3A6
CD184	APC	BDB	555976	12G5
CD29	APC	BDB	559883	MAR4
Mouse CD45	FITC	BDB	553080	30-F11
Mouse H-2Kd	FITC	BL	562003	SF1-1.1
Mouse CD41	FITC	BDB	553848	MWReg30
Mouse CD31	FITC	BDB	558738	390
Mouse CD31	FITC	BDB	553372	MEC13.3
Mouse CD71	FITC	BDB	553266	C2
Mouse Ter119	FITC	BDB	561032	TER-119
Live dead	Near-IR	Invitrogen	L10119	n/a
Live dead	Horizon FV510	BDB	564406	n/a

NOTE: Antibodies with mouse specificities were used as a species cocktail.
Abbreviations: BDB, BD Biosciences, San Jose, CA; BL, BioLegend, San Diego, CA; Mil, Miltenyi Biotec, Auburn, CA.

Published OnlineFirst December 30, 2016; DOI: 10.1158/1541-7786.MCR-16-0286-T

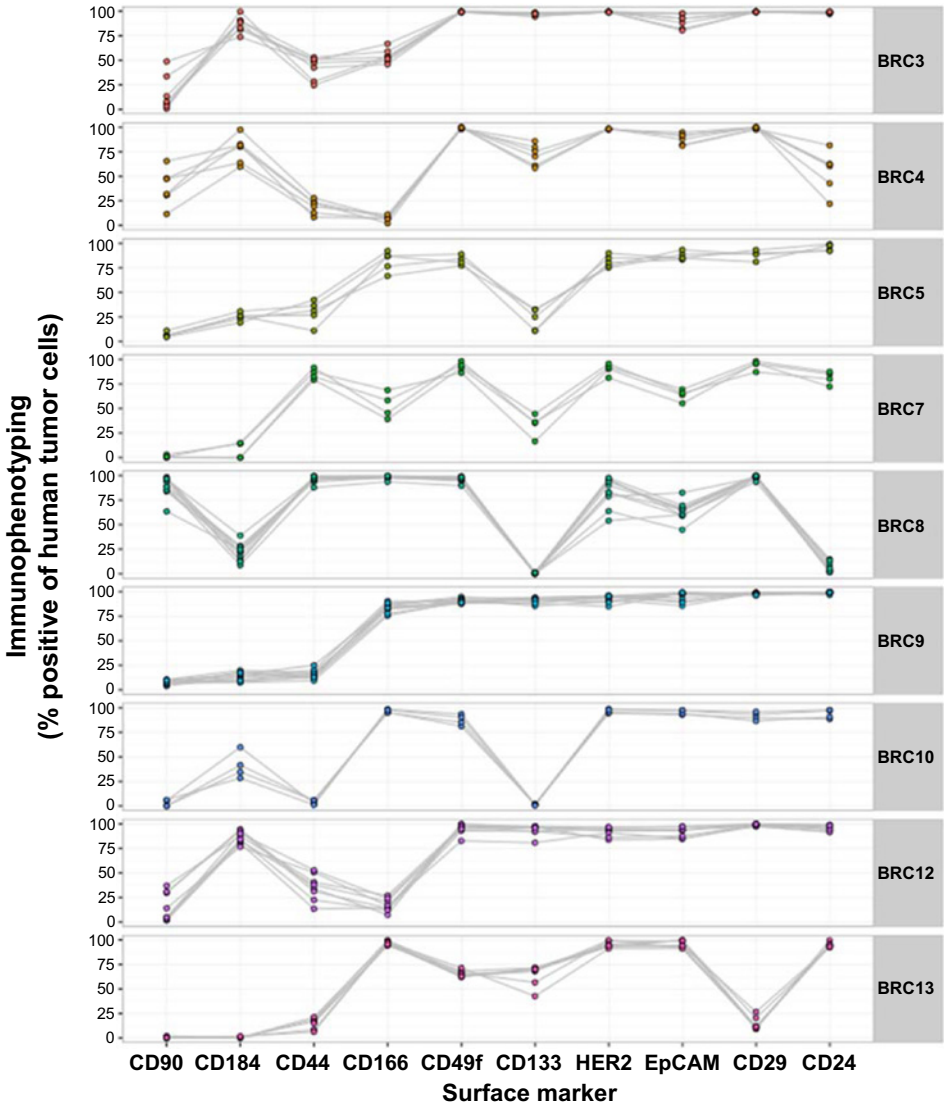

Figure 2.
Phenotyping of human breast tumor mouse models. BRC3–13 designate individual PDX cohorts (see Table 1). The *Y* axis indicates cells positive for each human marker in % of the human cell population for each cohort. Each dot represents one individual mouse; the number of mice analyzed per cohort ranges from 4 to 10.

the Kolmogorov–Smirnov test with the topGO R package: Adrian Alexa and Jorg Rahnenfuhrer (41).

Results

Flow cytometry analysis of PDX breast cancer biopsies

We analyzed human breast cancer cells obtained from 54 different PDX breast tumor biopsies (1 per mouse) from 9 different mouse cohorts by flow cytometry using a panel of 10 antibodies to human surface markers. The 9 cohorts were derived from 8 individual patients; BRC3 and -12 were different passages of the same original tumor model (Table 1). The antibody panel comprised surface markers previously identified on cell populations enriched in tumor-initiating cells or cells with enhanced metastatic capability or signs of epithelial–mesenchymal transition (EMT; refs. 26, 27, 29, 30, 42–44). We developed a gating strategy tailored for the detection of human markers on cells from tumor tissue excised from host mice. The percentage of cells positive for a given surface marker within all human cells of the excised tumor tissue was determined after successive exclusion of debris, dead cells, and cell aggregates as well as mouse cells from the events detected by the flow cytometry (Fig. 2 and Supplementary Fig. S1). Cell viability varied between cohorts and low viability generally correlated with signs of necrosis within a biopsy (data not shown).

These surface marker measurements provide an immunophenotypic profile for each PDX cohort which was reproducible and distinct among the different PDX tumor models (Fig. 2). The interpretation that this profile may be a specific and stable property of a given tumor is further supported by the high similarity between the profiles of BRC3 and -12—two passages of the same PDX tumor model (Figs. 2 and 3). In addition, the tumor sizes and times that different mice from each cohort were analyzed varied in a range that suggests that the stability of the profile also extends through much of the tumor development.

We built a model from this dataset using the 9 most significant surface markers and performed a distance tree categorical analysis that demonstrated that for 53 of the 54 individual tumors analyzed, each is grouped with the correct cohort (Fig. 3). Tumor T177 from BRC5 was an exception because the expression pattern

Published OnlineFirst December 30, 2016; DOI: 10.1158/1541-7786.MCR-16-0286-T

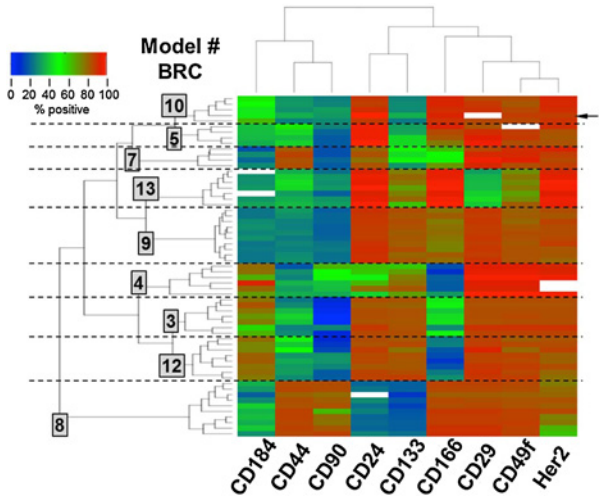

Figure 3.

Heatmap with distance tree displaying cluster analysis based on 9 markers for all 61 tumors. Numbers on the left indicate the point at which the respective cohort cluster splits off from its closest neighbor; position of the branch connector to the left reflects the degree of cluster difference (i.e., further left equals greater difference). The arrow marks the only tumor (T177, BRC5) which clusters outside of the cohort it was derived from. White boxes indicate the marker was not measured for the sample in question.

clustered with the closely related BRC10 cohort (marked by arrow in Fig. 3). A possible explanation is that CD29 was not measured for T177 and was missing for the clustering. Alternatively, adding other surface markers to the survey might allow further separation of individual cohorts.

A surprising finding was that clustering based on the surface markers chosen did not correlate well with their hormone receptor status. Although the BRC 5 and 10 (only non-TNB) clustered together as might be expected, the fact that several triple-negative (TN) cohorts (BRC 7, 9, 13) clustered more tightly with those two cohorts than with other TN cohorts (especially BRC8) is a direct indication of the intertumor heterogeneity of TN breast cancer. We did not observe any correlation between the immunophenotype and growth or tissue appearance (data not shown).

Next, we examined the dataset for pairwise correlations between markers. We performed permutation testing (10,000 permutations) for each pair of markers and adjusted the P values to correct for multiple testing in order to apply a meaningful statistical cutoff. As an example, we detected a negative correlation between the expression of CD24 and CD90 (Fig. 4; $R^2 = 0.77$; $P < 10^{-13}$). We investigated the 66 potential two-way correlations between the 10 human markers, fraction of murine cells in the biopsy, and % cell viability (Fig. 5). There was very low correlation of viability with any of the markers ($P > 0.05$), which is consistent with the notion that none of the surface markers is uniquely affected by our processing methods. On the other hand, 22 correlations (11 positive, 11 negative) proved to be statistically significant (two-tailed, alpha = 0.05), suggesting that the expression levels of several marker pairs are coordinated. This coordination would be consistent with both markers being regulated by connected cellular processes (e.g., proliferation, migration, etc.) because independent processes presumably lead to random co-occurrence.

Analysis of these correlations can thus generate specific hypotheses, and the surface marker surveys can contribute functional information in addition to the value as a categorization tool.

Transcriptional regulation in sorted cell populations

Profiling of PDX samples as described can be used as a tool in itself, but the data also revealed that each cancer analyzed here shows strong indications of ITH, which can be the starting point of deeper molecular investigations. Defined as the simultaneous presence of cells with and without a marker in question, ITH was

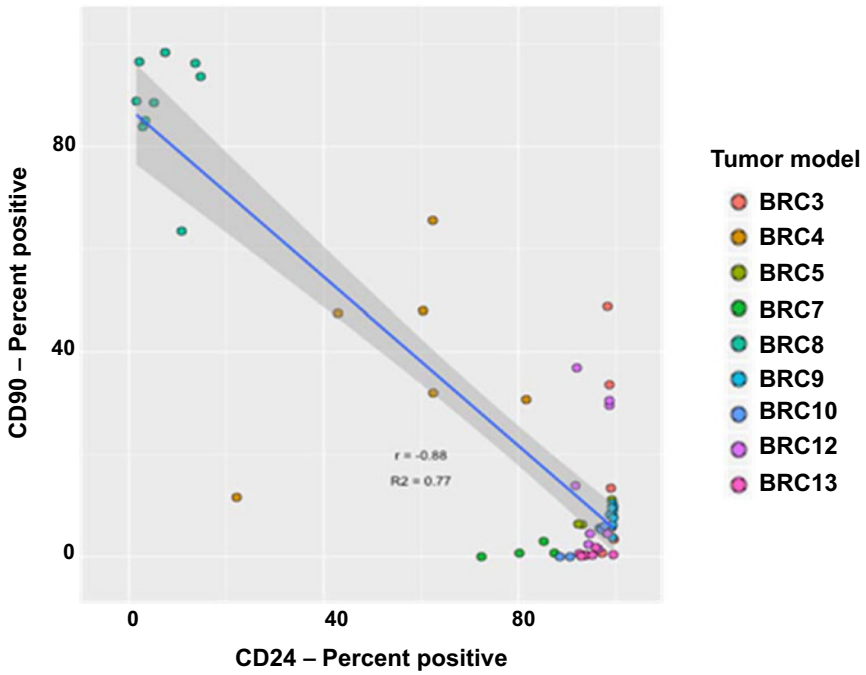

Figure 4.

Two-way correlation between marker expression levels (CD24 and CD90) in all cohorts. Each dot represents a biopsy from an individual mouse within one of the nine cohorts.

Published OnlineFirst December 30, 2016; DOI: 10.1158/1541-7786.MCR-16-0286-T

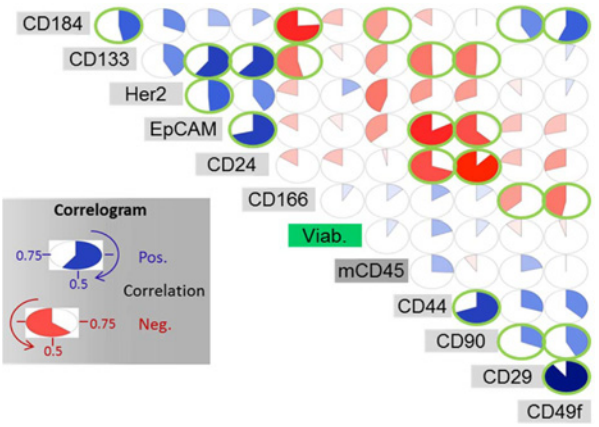

Figure 5.

Comprehensive Correlogram of all two-way correlations. The pie charts depict the R value (marked by circle filling and color intensity) for each pairwise correlation; blue = positive correlation; red = negative correlation. Correlations determined to be statistically significant (Supplementary Table S2) are marked with a green circle. Seven hundred thirty-two single-marker measurements (61 samples × 12 markers) were used.

detected in each cohort examined (Fig. 2). Interestingly, the markers which show such divisions varied among the cohorts. To investigate whether this immunophenotypic difference can reflect a more general subclonal organization of the tumor tissue, we chose one of the cohorts which reproducibly contained distinct populations either positive or negative for CD 184 (aka CXCR4) and positive for CD24. Both markers have been used to identify cells with CSC properties (25, 45) and our observation that distinct positive and negative populations for CD184 could be detected consistently in cohort BRC12. We subjected cells dissociated from tissue extracted from three different BRC12 mice to FACS sorting, creating four different cell pools from each mouse for RNA isolation: (1) unsorted bulk tumor cells; (2) bulk cells depleted of mouse cells; (3) $CD24^{+}/CD184^{lo}$ cells; and (4) $CD24^{+}/CD184^{hi}$ (Supplementary Fig. S2). RNASeq analysis on the whole transcriptome was performed, and gene expression differences were analyzed. A principal component analysis (PCA) of the entire dataset indicated a clear separation between populations based on species identity (PC2) and surface marker expression (PC1), which was very consistent among the triplicate samples (Fig. 6).

We compared our transcriptome data with a published dataset comprising 1,033 breast cancer samples of various intrinsic molecular subtypes (38). Our samples clustered with basal breast cancer, showing that the PDX subpopulations as well as the parent population retained the basal phenotype (Fig. 6B). However, subpopulations defined by CD184 surface expression showed major differences in their transcriptional profiles. We detected 1,197 genes which differed by more than 2-fold and below a false discovery rate (FDR) of 0.05, 246 of which were below FDR of 0.01. More intriguing even is the fact that most of these genes fell into a few distinct categories. Many of the genes highly expressed in the $CD184^{hi}$ cells are associated with cell proliferation, whereas genes overexpressed in the $CD184^{lo}$ pool are associated with regulatory processes within the cellular environment such as hypoxia, EMT, extracellular matrix (ECM) regulation, and angiogenesis (Fig. 6C). A group of genes known to be related to drug resistance in melanoma (46) showed significant upregulation on average in this pool as well (Fig. 7B), which is consistent with the notion that drug resistance is frequently associated with less proliferative cells and may point further to an important role of this subpopulation. Although these two distinct expression profiles reside in the same tumor tissue, the properties of the $CD184^{lo}$ subpopulation (see Fig. 2) would likely be undetectable in a bulk analysis.

A comprehensive analysis of the pathways upregulated in the respective populations expanded upon this finding; the pathways identified for $CD184^{hi}$ cells relate to cell proliferation. In contrast, the pathways active in the $CD184^{lo}$ population include downregulation of proliferation and are mostly related to extracellular communication, for example, ECM organization, cell–cell junction organization, and signal transduction (Fig. 7A).

Discussion

The utility of surface markers for identifying and isolating specific cell types of interest within tumor samples has been previously demonstrated (4, 8). These studies show the benefit of this approach, offering more detailed characterization and analysis than with conventional bulk methods (7, 23, 47). Our study shows that a systematic flow cytometry survey with an 11-color panel resulted in a novel characterization tool capable of phenotypically profiling a range of breast cancer samples beyond the current standard (e.g., hormone receptor status). This presents an opportunity especially for triple-negative breast cancers where there is a need for further subgrouping (31). Surface marker profiles may offer useful functionally relevant categorization with comparatively low resource commitment. We demonstrated that our method allows correct clustering of replicate PDX mice with similar and dissimilar tumors through analysis of their surface marker phenotype with high accuracy (Fig. 3). This finding indicates that the surface marker phenotype may be a reflection of tumor intrinsic properties which can be detected reproducibly by our methods. This notion is further supported by the tight clustering of BRC3 and BRC12, which represent two passages from the same model. Interestingly, the two cohorts which are not triple-negative breast cancer (TNB) models (BRC5 and BRC10) cluster very tightly as well, suggesting that there is overlap between hormone receptor/IHC-based categorization and surface marker patterns. Because all but two models investigated are TNB, our data do not support any strong conclusions on other breast cancer types. Surprising in this regard however is the finding that one of the TNB models (BRC8) has an immunophenotype that is unique from all the others, and the relationship between the other TNBs and the hormone receptor cohorts is closer than between BRC8 and any other cohort. This observation indicates either that surface immunophenotyping provides independent phenotypic information beyond the hormone receptor status or that PDX breast cancer models may not maintain their hormone receptor status detected in the patient material. Because 5% to 40% of breast cancer patients have discordant ER status when comparing metastases with primary lesions or among multiple primary foci (48), a switch in hormone receptor status during tumor graft development cannot be excluded.

A particular strength of the classification by immunophenotype is the ability to capture sample heterogeneity which is not reflected as exhaustively in any of the current classifications. IHC reveals a small amount of this information but is limited with regard to

Published OnlineFirst December 30, 2016; DOI: 10.1158/1541-7786.MCR-16-0286-T

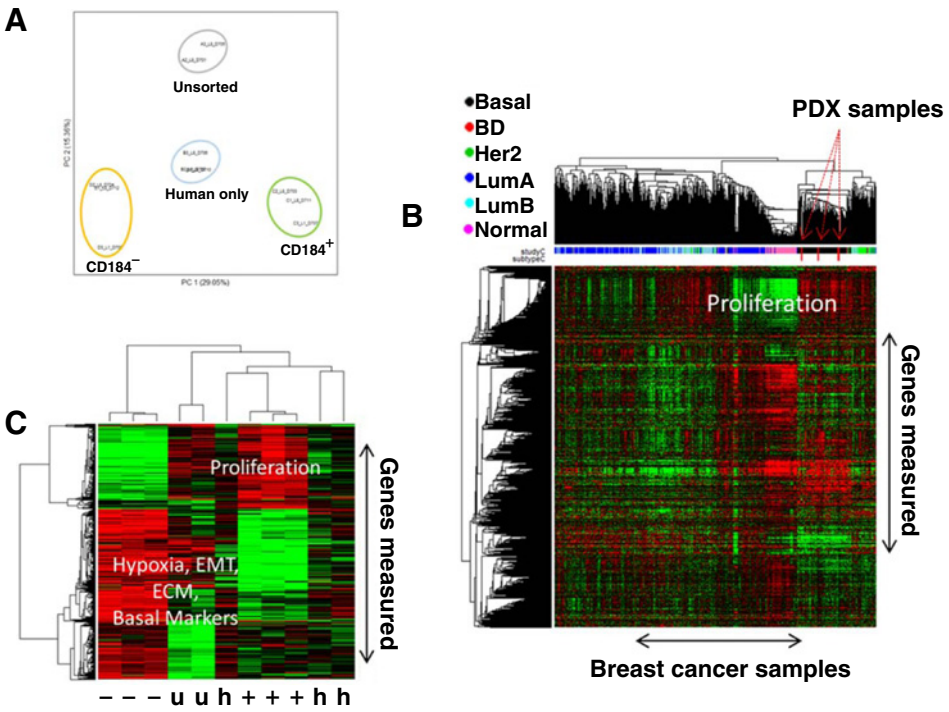

Figure 6.
PCA and cluster analysis of RNASeq data from sorted breast cancer cell populations. **A,** PCA for all populations. **B,** Cluster analysis for molecular subtyping of all sorted populations and 1,033 breast cancers in TCGA. **C,** Cluster analysis using gene subset; h, human; u, unsorted; −, CD184^{lo}; +, CD184^{hi}.

number of parameters and suitable objective metrics. Some classification systems (e.g., based on gene expression patterns) treat a biopsy as a clonal population, assigning a single-cell property to the entire tissue while more sophisticated sequencing methods may detect the presence of subclonal mutations, but only provide cell- or population-specific information with resource commitments prohibitive for medium to high sample throughput. In contrast, immunophenotyping specifically calls out the presence of subpopulations and their respective fraction within the sample. There are multiple recent studies demonstrating the functional relevance of these subpopulations, such as cell–cell communication within a cancer lesion, which further suggests that their assessment may have clinical importance (49–52). Use of a novel classification system reflecting on quantified heterogeneity seems very compelling. Supporting this argument is our finding of multiple statistically significant two-way correlations between markers which are consistent with coordinated cellular states rather than independent regulation of single entities. These correlations may spark new hypotheses and guide the search for relevant cellular pathways controlling specific states within the context of tumor development. Interestingly, one of the strongest negative correlations detected is CD24 or CD44 (Supplementary Table S2). Given that both markers have been found to be ambiguous with regard to their ability to identify CSCs (25), it is conceivable that in some cases (as in the original report of CD44^{+}CD24^{-} being a breast cancer CSC signature; ref. 4), the success of finding CSCs through a combination may be based on higher sensitivity with two antibodies rather than a bona fide role as CSC marker for both proteins.

Prompted by this apparent dynamic regulation of subpopulations, we performed a whole transcriptome analysis of subclones identified by the presence or absence of the cell surface chemokine receptor CD184 (CXCR4). This marker plays a role in tumor communication with the microenvironment (44), in metastasis (53), and intratumor communication (52). CXCR4/CD184 is also being pursued as cancer drug target (54). We identified distinct cell subpopulations, CD184^{hi} and CD184^{lo}, in our tumor model BRC12 (Supplementary Fig. S2) and performed gene expression analysis on the subpopulations. Although a comparison of the samples with a database of breast cancer–intrinsic subtypes grouped all within the basal breast cancer category, comparison between the CD184^{hi} and CD184^{lo} populations revealed stark contrasts in very specific cell signaling pathways. Proliferation-related genes were highly upregulated in cells expressing CD184, whereas the CD184^{lo} profile showed increased activity in ECM organization, angiogenesis, and promotion of differentiation of adjacent cell types. This contrast is consistent with the hypothesis that tumor tissue employs organizational elements present in healthy tissues to pursue various aspects of the hallmarks of cancer (55). Our observation that similar proportions of CD184^{hi} and CD184^{lo} populations were detected in two different passages of the same tumor model (BRC3 and BRC12; Fig. 2) supports the argument that these two subpopulations reflect a stable equilibrium. Reports by other investigators on more efficient engraftment of co-inoculation with CD184^{hi} and CD184^{lo} cells compared with either population alone and evidence for communication between those two populations (43, 52) support this view. Despite these demonstrations of the value of CD184, our results show variability in the proportion of CD184^{hi} cells. Thus, the nature of heterogeneity regarding CD184 is likely more complex and dependent on other factors. Further studies are needed to clarify the nature of this association.

The presence of a cell compartment with apparently slower proliferative capability, but high activity, in intercellular communication raises the interesting question whether diagnostics focusing on the most abundant cells may miss significant properties residing in a minority of the cells. The apparent coexistence of a slow and fast proliferating cell compartment also implies that the

Published OnlineFirst December 30, 2016; DOI: 10.1158/1541-7786.MCR-16-0286-T

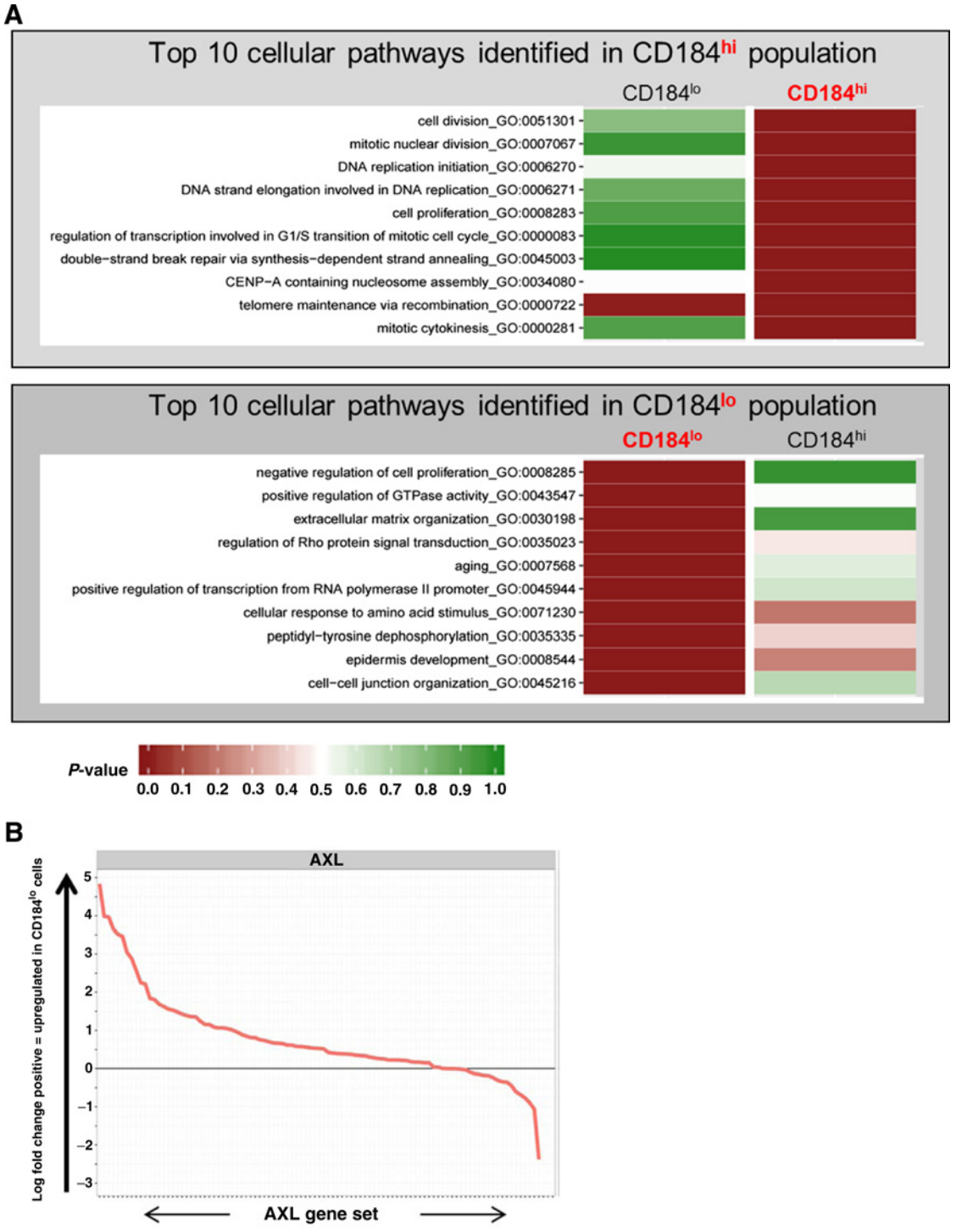

Figure 7.

A, Top 10 pathways (by *P* value) affected by gene expression differences between CD184^{hi} and CD184^{lo} cancer cells. Minimum *P* values on the list are 2.5×10^{-5} for CD184^{hi} and 2.6×10^{-4} for CD184^{lo}. **B,** Differential regulation of the AXL kinase gene set (38) between CD184^{lo} and CD184^{hi}cells (see Supplementary Table S2 for list of genes on the *x* axis).

tumor may use diverse strategies for greater resilience (56). Particularly any role in therapy resistance and recurrence warrants deeper investigation, and there are indeed numerous observations linking slower proliferating cells with drug resistance (57). The expression of 100 genes upregulated by the AXL kinase (Fig. 7B), which has been implicated in drug resistance in lung cancer and

melanoma (46), is significantly higher in $CD184^{lo}$ cells, adding a further facet to this picture.

Some specific gene expression differences further suggest a distinct role of the $CD184^{lo}$ compartment within the tumor tissue. Integrin beta 6 mRNA expression, which is 7.7-fold higher in this subpopulation, has been shown as an independent predictor of survival, and high expression is associated with distant metastasis and poor survival in breast cancer (58) as well as in colon cancer where it also appears to confer chemoresistance (59). A number of upregulated secreted factors with roles in cancer metastasis, angiogenesis, and hypoxia (e.g., TGFB1, LOXL4, WNT4) add to the interpretation that these cells communicate actively with their surrounding and may have a more significant role in the interaction with the TME than their $CD184^{hi}$ counterparts. Finally, overexpression of CD274 (PD-L1) (5.8-fold; FDR = 0.047) suggests $CD184^{lo}$ cells may also be more resilient against the host immune system.

Analysis of the bulk tissue (unsorted sample) did not reveal any of those properties, demonstrating that important traits in cancer biology are missed by the current standard.

Our results have to be interpreted within the context of the inherent limitations of a model system. Differences between the xenotransplantation host animal and the actual patient situation inevitably exist, most of all in the presence of an intact immune system interacting with the patient cancer tissue. The methods described here should allow to uncover powerful biological insights from patient biopsies, especially if the added heterogeneity of the immune cells can be included. On the other hand, the experimental control in the model system allows to establish some basic principles as shown in our study. Because similarities between cancer tissue from a PDX model and clinical samples are well documented (32), one can reasonably expect some of these principles to apply to the clinical situation. We believe our study forms an important building block on the way to cell subtype-specific studies which allow a comprehensive exploration of the cellular networks comprising clinical cancer tissues.

Conclusion

We have described novel single-cell–directed immunophenotyping methods for solid tumor cells. The deep immunophenotyping provides a new method of subtyping breast cancer cells. Most importantly, we have demonstrated that solid cancers can include cell subpopulations with substantial and biologically impactful differences compared with the whole population. These properties are undetectable with current standard methods based on bulk gene expression analysis. Our findings could have major implications for cancer biology and monitoring and predicting therapy response.

Disclosure of Potential Conflicts of Interest

S. Ghanekar is Associate Director at BD Biosciences. No potential conflicts of interest were disclosed by the other authors.

Authors' Contributions

Conception and design: E. Snowden, W. Porter, F. Hahn, A. Middlebrook, R. Blaesius

Development of methodology: F. Hahn, M. Ferguson, A. Middlebrook, S. Ghanekar, R. Blaesius

Acquisition of data (provided animals, acquired and managed patients, provided facilities, etc.): E. Snowden, W. Porter, F. Hahn, M. Ferguson

Analysis and interpretation of data (e.g., statistical analysis, biostatistics, computational analysis): E. Snowden, W. Porter, F. Hahn, F. Tong, J.S. Parker, A. Middlebrook, R. Blaesius

Writing, review, and/or revision of the manuscript: E. Snowden, W. Porter, F. Tong, J.S. Parker, S. Ghanekar, W.S. Dillmore, R. Blaesius

Administrative, technical, or material support (i.e., reporting or organizing data, constructing databases): E. Snowden, W. Porter, F. Hahn, M. Ferguson, A. Middlebrook

Study supervision: W.S. Dillmore, R. Blaesius

The costs of publication of this article were defrayed in part by the payment of page charges. This article must therefore be hereby marked *advertisement* in accordance with 18 U.S.C. Section 1734 solely to indicate this fact.

Received August 26, 2016; revised November 23, 2016; accepted December 21, 2016; published OnlineFirst December 30, 2016.

References

1. Ross JS, Schenkein DP, Pietrusko R, Rolfe M, Linette GP, Stec J, et al. Targeted therapies for cancer 2004. Am J Clin Pathol 2004;122:598–609.
2. Groenendijk FH, Bernards R. Drug resistance to targeted therapies: Deja vu all over again. Mol Oncol 2014;8:1067–83.
3. Hanahan D, Coussens LM. Accessories to the crime: Functions of cells recruited to the tumor microenvironment. Cancer Cell 2012;21:309–22.
4. Al-Hajj M, Wicha MS, Benito-Hernandez A, Morrison SJ, Clarke MF. Prospective identification of tumorigenic breast cancer cells. Proc Natl Acad Sci U S A 2003;100:3983–8.
5. Chen J, Li Y, Yu TS, McKay RM, Burns DK, Kernie SG, et al. A restricted cell population propagates glioblastoma growth after chemotherapy. Nature 2012;488:522–6.
6. Kamel-Reid S, Letarte M, Sirard C, Doedens M, Grunberger T, Fulop G, et al. A model of human acute lymphoblastic leukemia in immune-deficient SCID mice. Science 1989;246:1597–600.
7. Ruffell B, Au A, Rugo HS, Esserman LJ, Hwang ES, Coussens LM. Leukocyte composition of human breast cancer. Proc Natl Acad Sci U S A 2012;109:2796–801.
8. Chaffer CL, Brueckmann I, Scheel C, Kaestli AJ, Wiggins PA, Rodrigues LO, et al. Normal and neoplastic nonstem cells can spontaneously convert to a stem-like state. Proc Natl Acad Sci U S A 2011;108:7950–5.
9. Kreso A, Dick JE. Evolution of the cancer stem cell model. Cell Stem Cell 2014;14:275–91.
10. Nowell PC. The clonal evolution of tumor cell populations. Science 1976;194:23–8.
11. Heppner GH, Miller BE. Tumor heterogeneity: biological implications and therapeutic consequences. Cancer Metastasis Rev 1983;2:5–23.
12. Maley CC, Galipeau PC, Finley JC, Wongsurawat VJ, Li X, Sanchez CA, et al. Genetic clonal diversity predicts progression to esophageal adenocarcinoma. Nat Genet 2006;38:468–73.
13. Marusyk A, Polyak K. Tumor heterogeneity: causes and consequences. Biochim Biophys Acta 2010;1805:105–17.
14. Dalerba P, Kalisky T, Sahoo D, Rajendran PS, Rothenberg ME, Leyrat AA, et al. Single-cell dissection of transcriptional heterogeneity in human colon tumors. Nature Biotechnology 2011;29:1120–7.
15. Shipitsin M, Campbell LL, Argani P, Weremowicz S, Bloushtain-Qimron N, Yao J, et al. Molecular definition of breast tumor heterogeneity. Cancer cell 2007;11:259–73.
16. Morris LG, Riaz N, Desrichard A, Senbabaoglu Y, Hakimi AA, Makarov V, et al. Pan-cancer analysis of intratumor heterogeneity as a prognostic determinant of survival. Oncotarget 2016;7:10051–63.
17. Burrell RA, Swanton C. Tumour heterogeneity and the evolution of polyclonal drug resistance. Mol Oncol 2014;8:1095–111.
18. Su K-Y, Chen H-Y, Li K-C, Kuo M-L, Yang JC-H, Chan W-K, et al. Pretreatment epidermal growth factor receptor (EGFR) T790M mutation predicts shorter EGFR tyrosine kinase inhibitor response duration

Published OnlineFirst December 30, 2016; DOI: 10.1158/1541-7786.MCR-16-0286-T

in patients with non-small-cell lung cancer. J Clin Oncol 2012; 30:433–40.
19. Schmitt MW, Loeb LA, Salk JJ. The influence of subclonal resistance mutations on targeted cancer therapy. Nat Rev Clin Oncol 2016;13: 335–47.
20. Chung GG, Zerkowski MP, Ghosh S, Camp RL, Rimm DL. Quantitative analysis of estrogen receptor heterogeneity in breast cancer. Lab Invest 2007;87:662–9.
21. Klco JM, Spencer DH, Miller CA, Griffith M, Lamprecht TL, O'Laughlin M, et al. Functional heterogeneity of genetically defined subclones in acute myeloid leukemia. Cancer Cell 2014;25:379–92.
22. Dunleavey JM, Xiao L, Thompson J, Kim MM, Shields JM, Shelton SE, et al. Vascular channels formed by subpopulations of PECAM1(+) melanoma cells. Nat Commun 2014;5:5200.
23. Gedye CA, Hussain A, Paterson J, Smrke A, Saini H, Sirskyj D, et al. Cell surface profiling using high-throughput flow cytometry: A platform for biomarker discovery and analysis of cellular heterogeneity. PLoS One 2014;9:e105602.
24. Alizadeh AA, Aranda V, Bardelli A, Blanpain C, Bock C, Borowski C, et al. Toward understanding and exploiting tumor heterogeneity. Nat Med 2015;21:846–53.
25. Jaggupilli A, Elkord E. Significance of CD44 and CD24 as cancer stem cell markers: An enduring ambiguity. Clin Dev Immunol 2012;2012: 708036.
26. Leccia F, Nardone A, Corvigno S, Vecchio LD, De Placido S, Salvatore F, et al. Cytometric and biochemical characterization of human breast cancer cells reveals heterogeneous myoepithelial phenotypes. Cytometry A 2012;81:960–72.
27. Pattabiraman DR, Weinberg RA. Tackling the cancer stem cells - what challenges do they pose? Nat Rev Drug Discov 2014;13:497–512.
28. Perez EA, Cortes J, Gonzalez-Angulo AM, Bartlett JM. HER2 testing: Current status and future directions. Cancer Treat Rev 2014;40:276–84.
29. Vassilopoulos A, Chisholm C, Lahusen T, Zheng H, Deng CX. A critical role of CD29 and CD49f in mediating metastasis for cancer-initiating cells isolated from a Brca1-associated mouse model of breast cancer. Oncogene 2014;33:5477–82.
30. Weidle UH, Eggle D, Klostermann S, Swart GW. ALCAM/CD166: Cancer-related issues. Cancer Genomics Proteomics 2010;7:231–43.
31. Turner NC, Reis-Filho JS. Tackling the diversity of triple-negative breast cancer. Clin Cancer Res 2013;19:6380–8.
32. Simpson-Abelson MR, Sonnenberg GF, Takita H, Yokota SJ, Conway TFJr, Kelleher RJJr, et al. Long-term engraftment and expansion of tumor-derived memory T cells following the implantation of non-disrupted pieces of human lung tumor into NOD-scid IL2Rgamma(null) mice. J Immunol 2008;180:7009–18.
33. Kreso A, O'Brien CA, van Galen P, Gan O, Notta F, Brown AM, et al. Variable clonal repopulation dynamics influence chemotherapy response in colorectal cancer. Science 2012;339:543–8.
34. Pechoux C, Gudjonsson T, Ronnov-Jessen L, Bissell MJ, Petersen OW. Human mammary luminal epithelial cells contain progenitors to myoepithelial cells. Dev Biol 1999;206:88–99.
35. O'Hare MJ, Ormerod MG, Monaghan P, Lane EB, Gusterson BA. Characterization in vitro of luminal and myoepithelial cells isolated from the human mammary gland by cell sorting. Differentiation 1991;46:209–21.
36. McDivitt RW, Stone KR, Meyer JS. A method for dissociation of viable human breast cancer cells that produces flow cytometric kinetic information similar to that obtained by thymidine labeling. Cancer Res 1984;44:2628–33.
37. R Core Team (2015). R: A language and environment for statistical computing. R Foundation for Statistical Computing, Vienna, Austria. https://www.R-project.org/.
38. Cancer Genome Atlas N. Comprehensive molecular portraits of human breast tumours. Nature 2012;490:61–70.
39. van Iersel MP, Kelder T, Pico AR, Hanspers K, Coort S, Conklin BR, et al. Presenting and exploring biological pathways with PathVisio. BMC Bioinformatics 2008;9:399.
40. Kutmon M, van Iersel MP, Bohler A, Kelder T, Nunes N, Pico AR, et al. PathVisio 3: An extendable pathway analysis toolbox. PLoS Comput Biol 2015;11:e1004085.
41. topGO: Enrichment Analysis for Gene Ontology. R package version 2.24.0.
42. Davies S, Jiang WG. ALCAM, activated leukocyte cell adhesion molecule, influences the aggressive nature of breast cancer cells, a potential connection to bone metastasis. Anticancer Res 2010;30:1163–8.
43. Luker KE, Lewin SA, Mihalko LA, Schmidt BT, Winkler JS, Coggins NL, et al. Scavenging of CXCL12 by CXCR7 promotes tumor growth and metastasis of CXCR4-positive breast cancer cells. Oncogene 2012;31:4750–8.
44. Orimo A, Gupta PB, Sgroi DC, Arenzana-Seisdedos F, Delaunay T, Naeem R, et al. Stromal fibroblasts present in invasive human breast carcinomas promote tumor growth and angiogenesis through elevated SDF-1/CXCL12 secretion. Cell 2005;121:335–48.
45. Mukherjee S, Manna A, Bhattacharjee P, Mazumdar M, Saha S, Chakraborty S, et al. Non-migratory tumorigenic intrinsic cancer stem cells ensure breast cancer metastasis by generation of CXCR4+ migrating cancer stem cells. Oncogene 2016;35:4937–48.
46. Tirosh I, Izar B, Prakadan SM, Wadsworth MH, Treacy D, Trombetta JJ, et al. Dissecting the multicellular ecosystem of metastatic melanoma by single-cell RNA-seq. Science 2016;352:189–96.
47. Kronig M, Walter M, Drendel V, Werner M, Jilg CA, Richter AS, et al. Cell type specific gene expression analysis of prostate needle biopsies resolves tumor tissue heterogeneity. Oncotarget 2015;6:1302–14.
48. Baretta Z, Olopade OI, Huo D. Heterogeneity in hormone-receptor status and survival outcomes among women with synchronous and metachronous bilateral breast cancers. Breast 2015;24:131–6.
49. Archetti M, Ferraro DA, Christofori G. Heterogeneity for IGF-II production maintained by public goods dynamics in neuroendocrine pancreatic cancer. Proc Natl Acad Sci U S A 2015;112:1833–8.
50. Cleary AS, Leonard TL, Gestl SA, Gunther EJ. Tumour cell heterogeneity maintained by cooperating subclones in Wnt-driven mammary cancers. Nature 2014;508:113–7.
51. Polyak K, Marusyk A. Cancer: Clonal cooperation. Nature 2014;508:52–3.
52. Zhang M, Tsimelzon A, Chang CH, Fan C, Wolff A, Perou CM, et al. Intratumoral heterogeneity in a Trp53-null mouse model of human breast cancer. Cancer Discov 2015;5:520–33.
53. Muller A, Homey B, Soto H, Ge N, Catron D, Buchanan ME, et al. Involvement of chemokine receptors in breast cancer metastasis. Nature 2001;410:50–6.
54. Cojoc M, Peitzsch C, Trautmann F, Polishchuk L, Telegeev GD, Dubrovska A. Emerging targets in cancer management: Role of the CXCL12/CXCR4 axis. Onco Targets Ther 2013;6:1347–61.
55. Hanahan D, Weinberg RA. Hallmarks of cancer: The next generation. Cell 2011;144:646–74.
56. Aktipis CA, Boddy AM, Gatenby RA, Brown JS, Maley CC. Life history trade-offs in cancer evolution. Nat Rev Cancer 2013;13:883–92.
57. Schillert A, Trumpp A, Sprick MR. Label retaining cells in cancer–the dormant root of evil? Cancer Lett 2013;341:73–9.
58. Moore KM, Thomas GJ, Duffy SW, Warwick J, Gabe R, Chou P, et al. Therapeutic targeting of integrin alphavbeta6 in breast cancer. J Natl Cancer Inst 2014;106.
59. Liang B, Shahbaz M, Wang Y, Gao H, Fang R, Niu Z, et al. Integrinbeta6-targeted immunoliposomes mediate tumor-specific drug delivery and enhance therapeutic efficacy in colon carcinoma. Clin Cancer Res 2015;21:1183–95.

AACR American Association for Cancer Research

Molecular Cancer Research

Immunophenotyping and Transcriptomic Outcomes in PDX-Derived TNBC Tissue

Eileen Snowden, Warren Porter, Friedrich Hahn, et al.

Mol Cancer Res Published OnlineFirst December 30, 2016.